Halogens molecular modifications with high pressure: the case of iodine Supplemental Material

Jingming Shi,[1,2] Emiliano Fonda,[3] Silvana Botti,[4,5] Miguel A. L. Marques,[6,5] Toru Shinmei,[7] Tetsuo Irifune,[7,8] Emiliano Fonda,[3] Anne-Marie Flank,[3] Pierre Lagarde,[3] Alain Polian,[3,9] Jean-Paul Itié,[3] and Alfonso San-Miguel[1,*]

[1] *Univ Lyon, Université Claude Bernard Lyon 1, CNRS, Institut Lumière Matière, F-69622 LYON, France*
[2] *School of Physics and Electronic Engineering, Jiangsu Normal University, Xuzhou 221116,China*
[3] *Synchrotron SOLEIL, L'Orme des Merisiers, Saint-Aubin, BP48, 91192 Gif-sur-Yvette Cedex, France*
[4] *Institut für Festkörpertheorie und -optik, Friedrich-Schiller-Universität Jena, Max-Wien-Platz 1, 07743 Jena, Germany*
[5] *European Theoretical Spectroscopy Facility*
[6] *Institut für Physik, Martin-Luther-Universität Halle-Wittenberg, D-06099 Halle, Germany*
[7] *Geodynamics Research Center, Ehime University, Matsuyama, Ehime 790-8577, Japan*
[8] *Earth-Life Science Institute, Tokyo Institute of Technology, Tokyo 152-8550, Japan*
[9] *IMPMC-CNRS UMR 7590, Sorbonne Université, B115, 4 place Jussieu, F-75252 Paris Cedex 05, France*

I. EXPERIMENTAL METHODS

Four different high pressure X-ray absorption spectroscopy (XAS) experiments were performed at the L_I(5.19 keV), L_{III}(4.56 keV) and K-edges(33.17 keV) (see Table I). Two types of pressure apparatus were used, namely a diamond anvil cell (DAC) and a Paris-Edinburgh press.[1] Diamond anvils included mini-anvils (thickness = 0.5 mm) supported by perforated ones[2] to reduce X-ray absorption in the L_I and L_{III}-edge experiments or nanopolycrystalline anvils[3] to avoid the introduction of X-ray diffraction glitches in the absorption spectra at the higher energy K-edge. Iodine K-edge high pressure experiments were performed at the SAMBA beamline of the SOLEIL synchrotron (Saclay, France) and at the BM29 beamline of the European synchrotron Radiation Facility (ESRF,Grenoble, France). Iodine L_I- and L_{III}-edge high pressure experiments were done at the LUCIA beamline in its configuration at SLS(Villigen, Switzerland) and SOLEIL (Saclay, France). Pressure was measured either from the ruby-shift secondary scale or calibrated from diffraction data of pressure calibrants or from iodine itself. To avoid contamination of the highly hygroscopic iodine, pressure loading was always done using glove-bags in an inert nitrogen or argon atmosphere. All experiments were done at ambient temperature, but loading in the different pressure cells was done at liquid nitrogen temperature. More information on the different types of experimental set-up used in our work can be found in review articles about XAS at high pressure[4,5]

K-edge high pressure XAS spectra at the SAMBA beamline (SOLEIL) were obtained in a step by step acquisition scheme in transmission mode. The X-ray optics includes a sagittal focusing Si (220) double monochromator placed between two bendable cylindrical mirrors. This allows to obtain a 200x300 μm^2 spot in the sample hutch which was further slitted down to avoid signal from the metallic gasket. Two ionization chambers were placed before and after the sample for the detection of the incoming and the transmitted beam through the sample. The sample X-ray diffraction pattern was also measured by placing a MAR 2D detector at $\sim$ 45 cm after the sample.More details on the experimental set-up can be found elsewhere.[6] Typical acquisition time for a single spectrum was 45 minutes. For each pressure point 6 spectra were averaged which allowed to obtain high quality data. At each pressure point angular dispersive diffraction patterns were recorded before and after the XAS acquisition. A total of six hours was needed to collect one pressure point allowing the acquisition of 12 pressure points. Nanopolycrystalline anvils[3] were used to avoid the introduction of X-ray diffraction glitches in the absorption spectra. Pressure was measured from the ruby-shift in the first pressure points but the weak ruby signal was finally lost. No pressure transmitting medium was used. Pressure was then calibrated from the diffraction data, except for the last spectrum for which the signal was lost. The maximum reached pressure was of more than 30 GPa. Examples of EXAFS signal are shown in Fig. S1.

K-edge high pressure XAS spectra at the BM29 beamline (ESRF) were also obtained in a step by step acquisition scheme in transmission mode using a nitrogen cooled Si (311) double crystal monochromator and a double mirror for harmonic rejection and vertical focusing (Pt stripe at 2 mrad). High pressure was generated using a Paris-Edinburgh press. The X-ray beam goes then through amorphous boron-epoxy gaskets which do not introduce diffraction glitches. In order to optimize the effective iodine thickness to a value of $\sim$84 μm iodine was mixed in a 1:9 proportion with a h-BN powder. A separate layer of NaCl was also included to allow for pressure calibration using X-ray diffraction detected with a MAR345 image plate.The maximum pressure reached was 12.1 GPa.

The L_I and L_{III} experiments presented here were done at the LUCIA beamline at SOLEIL using Si (111) doubled monochromator combined with a Kirckpatrick-Baez double mirror focusing system with a detection in transmission. A DAC with fully perforated anvils with mini-

* alfonso.san-miguel@univ-lyon1.fr

Iodine Edge	Synchrotron facility/Beamline	High pressure device	Pressure transmitting medium
K-edge	SOLEIL/SAMBA	nanopolycrytalline DAC	none
K-edge	ESRF/BM29	Paris-Edinburgh press	BN powder
L_I and L_{III} edge	SOLEIL/LUCIA	perforated DAC	none
L_I and L_{III} edge	SLS/LUCIA	perforated DAC	BN powder

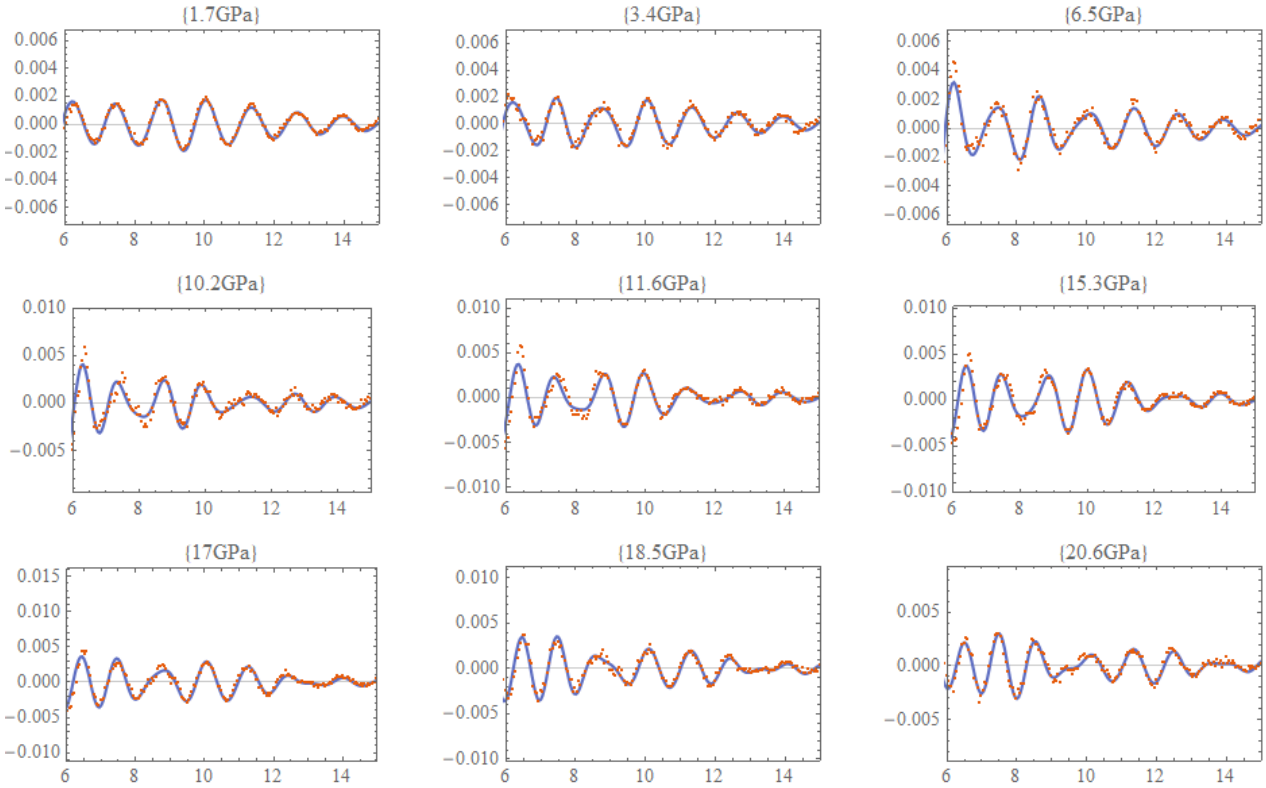

FIG. S1. Iodine K-edge EXAFS data fits ($k^3\chi(k)$ as function of k (Å^{-1}) for the different pressures. Red dots are the EXAFS data and blue lines correspond to the best fit. Data from the SOLEIL SAMBA K-edge experiment.

anvils on top (2x5 mm) was used as pressure apparatus in order to reduce the X-ray attenuation from the diamond anvils at these low energies. A similar experiment was also done in the LUCIA beamline set-up at SLS (Switzerland) synchrotron with an estimated maximum pressure of 27 GPa. In this experiment iodine was mixed with h-BN powder to optimize the XAS signal and a similar sequence of XANES spectra were obtained with respect to the LUCIA/SOLEIL experiment in which no pressure transmitting medium was used. The data of this experiment is not presented as the pressure could only be estimated from the applied pressure on the membrane of the DAC as the ruby signal was lost from the beginning of the experiment.

II. SUPPLEMENTARY FIGURES FROM EXPERIMENTS

Figure S2 shows that the L1-edge pre-peak characteristic of the sigma antibonding density of states shows a full width at half maximum (FWHM) change in the 7-10 GPa which can be associated to the intramolecular change of regime. The same behavior was obtained in bromine at the K-edge, which follows the same dipolar selection rule and allows visibility of the pre-peak due to the lower energy of the K-edge in bromine.

III. XANES AND EXAFS DATA ANALYSIS

XANES spectra from all experiments were normalized using the CDXAS code[7] and good agreement between the different experiments at the same iodine edge was obtained. EXAFS analysis was only possible for the two experiments done at the iodine K-edge. The EXAFS data extraction and analysis was done using FEFF[8] and FEFFIT[9] respectively.

The EXAFS analysis to obtain the intra-molecular distance was only possible on the K-edge data. The EXAFS analysis protocol described below was applied to the two K-edge experiments. Nevertheless, we realized that

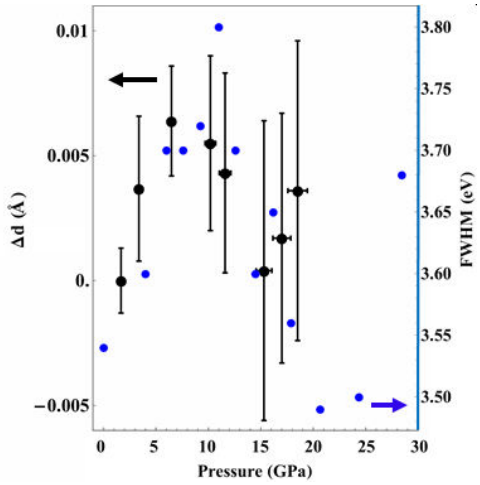

FIG. S2. Blue circles(right vertical axis): Pressure evolution of the L_I-edge pre-peak FWHM showing a change of behavior in the 7 - 10 GPa range. We observe another change of behavior between 25 and 30 GPa in good agreement with the expected phase transition towards phase II.Black circles: Obtained evolution of the intramolecular distance (see manuscript). The good correlation between the two independent measurements in two different experiments can be easily appreciated.

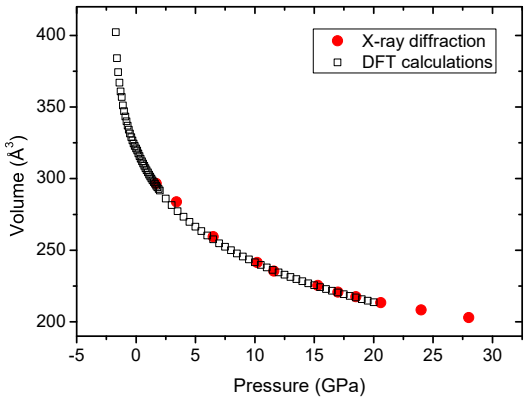

FIG. S3. Atomic volume obtained from our DFT calculations compared to our X-ray diffraction results.

the EXAFS signal at equivalent pressures were not in very good correspondence between the two experiments. In addition, fits for the K-edge data obtained in the BM29(ESRF) experiment were significantly worst that from the SAMBA(SOLEIL) experiment. Due to the complex environment of the BM29(ESRF) experiment using the Paris-Edinburgh press with BN and NaCl media, we suspect a contamination of the iodine sample and decided to exclude that data for the analysis. We discuss below the data analysis for the SAMBA (SOLEIL) experiments using DAC and no pressure transmitting medium.

EXAFS signal was extracted using Athena from the Demeter XAS analysis package[10] with a cutoff for background substraction set at k=1.5 Å^{-1}. Self-consistent potential calculations were used to generate the photoelectron scattering paths with the FEFF code[11] using the iodine *Cmca* crystal structure obtained by the *in situ* diffraction experiments at each pressure.A total of 7 scattering paths were used in the fit (the use of more scattering paths did not affect the fit and even self consistency was found not to affect the fit). The k-range domain for the EXAFS fit was set considering the goodness of fit for the first pressure spectrum which is strongly dominated by the intramolecular scattering path. It was found that for k <6 Å^{-1} there was a strong fit degradation which was not possible to solve. This fit problem in the low-k domain was partially solved by increasing the number of scattering paths in the fit. When introducing 23 scattering paths including multiple scattering ones, the low-k domain was in fact better fitted, but the whole quality of the fit was lowered. The fitting k-domain was then set between 6 and 15 Å^{-1} in order to obtain more reliable results, not depending on the number of multiple scattering paths participating to the fit. The constant amplitude factor, S_0 and shift of energy origin, e_0 were fixed from the values obtained from the fit of the first pressure spectrum. A Mathematica code was used to run FEFFIT with paths corresponding to the diffraction structure of each pressure point. Only the intramolecular path was kept constant for all pressures. The fitting parameters were the intra-molecular distance and an adjustment of the scale factor on the rest of the structure as well as pseudo Debye temperature factors for that same both "distances". Fits were done in r-space from the Fourier transformed $k^3\chi(k)$ EXAFS signal, in a domain from 1.9 to 4.0 Å. We may note that the fact of introducing a higher number of scattering paths in the fit did not affect the obtained evolution of the intramolecular distance, which appeared to be a very stable result. The EXAFS data at 20.6 GPa and 24 GPa could still be fitted within the Cmcm low pressure phase-I, but the fit quality started to be worst. This fact associated to changes in the XANES region and an important shift in the iodine intramolecular distance, indicate the probable presence of phase mixing at this two pressure points, in good correspondence with the iodine phase diagram. All our attempts to fit the last pressure EXAFS data at more than 30 GPa failed. We also suspect phase mixing and probably a phase opposition between the first two neighbor contributions leading to a cancellation of their signal in the pseudo-radial distribution function (PRDF). The high intensity peak in the PRDF may then probably correspond to the contribution of 3rd neighbors in the regions of mixing phases in the phase diagram.

IV. THEORETICAL METHODS

Ab initio calculations were performed using density functional theory implemented in the Quantum

TABLE S1. Structural information of I_2 in *Cmca* phase from DFT calculations using the PBE exchange-correlation functional and different correction for van der waals interactions. The lattice parameters and volume are in Å and Å^3, respectively.

persudo potential	a	b	c	Volume
Experiment	7.103	4.632	9.789	322.12
PBE_vdw-DF	7.703	4.813	9.821	364.23
PBE_vdw-DF2	7.536	4.830	9.868	359.27
PBE_vdW-DF-obk8	7.244	4.547	9.744	321.02
PBE_vdW-DF-ob86	7.175	4.471	9.708	311.47
PBE_vdw-DF-c09	7.013	4.386	9.649	296.86

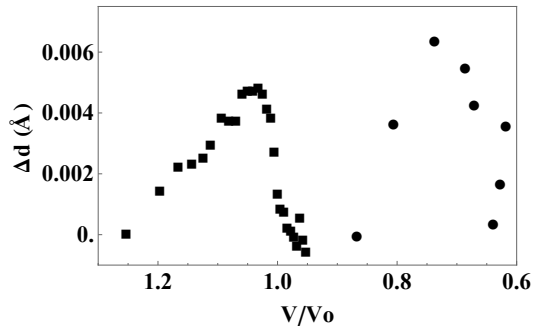

FIG. S4. Intramolecular distance evolution as function of the normalized volume V/V_0 from experiments(circles) and modelling (squares).Pressure to volume conversion of the experimental data is done through the iodine phase I equation of state.

ESPRESSO package,[12] with Norm-Conserving Perdew-Burke-Ernzenhof[13] (PBE) pseudopotential. Using the PWscf code, we performed ground-state total energy calculations under different hydrostatic pressures. During structrual optimization, we include van der Waals interactions through the modified VDW-DF-OBK8 functional.[14,15] The kinetic-energy cutoff for the wavefunctions was set at 80 Ry for our calculations. We used an automatically generated uniform Monkhorst–Pack k-points grid of $6 \times 8 \times 6$ points for the *Cmca* structure of iodine; The convergence threshold for ionic minimization on residual Hellmann–Feynman forces was 10^{-8} a.u..

V. CHLORINE CUSP PRESSURE DETERMINATION AND SCALED VOLUME DETERMINATION

In Fig. 4c of the main article, we have proposed a determination of the scaled volume, $\tilde{V(P)} = V(P)/(r(P)^3)$, evolution of chlorine, This evolution is determined under the following constraints:

- The atomic volume, $V(P)$, evolution is taken from the equation of state from Ref. 16.
- The intramoleculacular distance, $r(P)$ evolves in the following way modelling the observed evolution of iodine and bromine:

$$\left\{\begin{array}{c} r(P) = r_0 + \alpha P \ \text{ for } P \leq P_c \\ r(P) = r_0 + \alpha P_c - \beta\alpha(P - P_c) \ \text{ for } P \geq P_c \end{array}\right\} \quad (1)$$

- We set the metallization pressure at the iodine metallization one of 14 GPa,[17] which gives a metallization scaled volume of 1.55 ± 0.02.
- In Ref. 16, chlorine metallization is found at 200 GPa.
- For the cusp pressure, the scaled volume is of 1.55 ± 0.02
- The rates of expansion α for iodine and bromine are vary between 0.2 and 0.4% up to the cusp pressure.

Under these constraints we are able to determine a series of α, β and P_c as given in the main article text.

VI. SUPPLEMENTARY FIGURES FROM CALCULATIONS

A. High pressure evolution of structural parameters

Fig. **??** and Fig. **??** show respectively the evolution with pressure of interatomic distances and intermolecular angles as obtained from our DFT calculations.

B. Density of state difference (DOSD)

Fig. S6 shows the density of state difference (DOSD) of *Cmca* phase of iodine at different pressures with respect to the DOSD calculated at -1 GPa. We can clearly find that the DOS change becomes noticeable at -0.4 GPa. Beyond -0.2 GPa, as pressure further increases the amplitude of the signal does not evolve significantly. These observations are in good agreement with the evolution of the charge density difference variation as function of pressure revealing that at the cusp pressure operates a change in the electronic structure associated to bond formation between iodine molecules distant of (r_2).

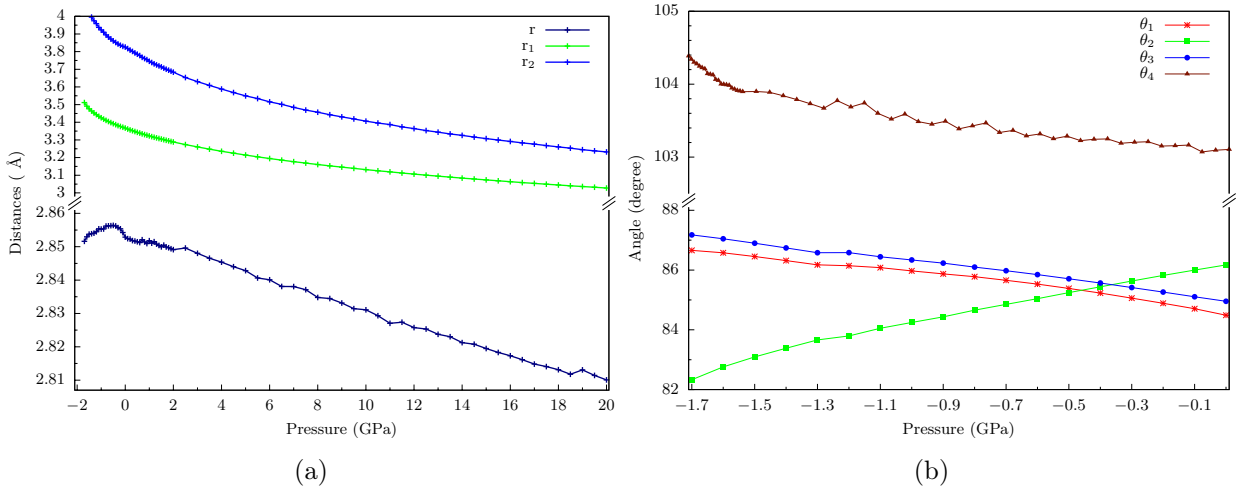

FIG. S5. (a), Interatomic distances obtained from our DFT calculations for the first 3 neighbor shells. (b), Intermolecular angles variation as a function of pressure. (The labels for the angel are illustrated in the Fig.1 in the main text)

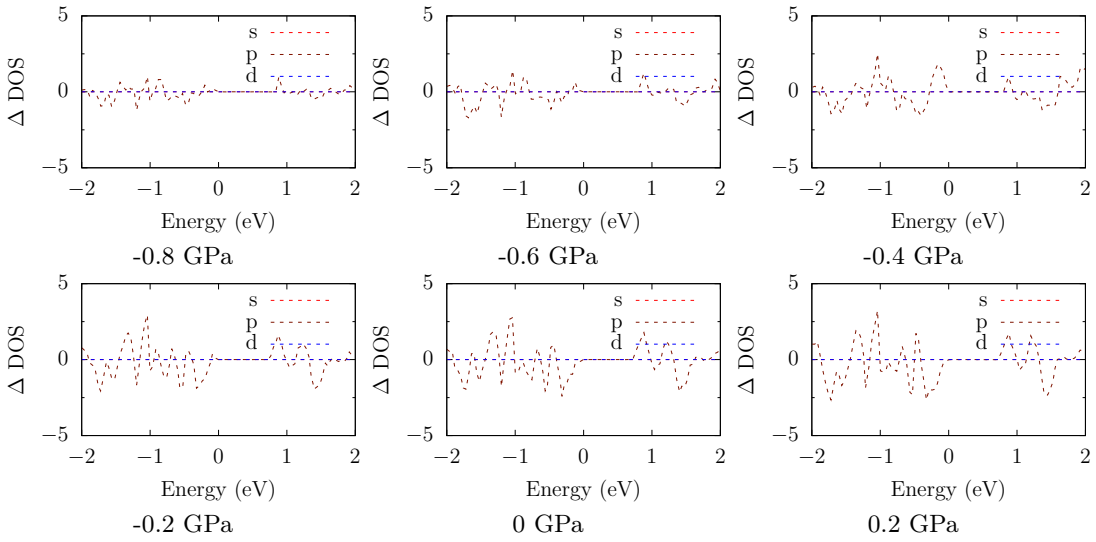

FIG. S6. The density of state difference (DOSD) plots of *Cmca* phase of iodine at selected pressures with respected to values of -1 GPa.

[1] G. Morard, M. Mezouar, N. Rey, R. Poloni, A. Merlen, S. L. Floch, P. Toulemonde, S. Pascarelli, A. San-Miguel, C. Sanloup, and G. Fiquet, High Pressure Research **27**, 223 (2007), https://doi.org/10.1080/08957950601183553.

[2] J.-P. Itié, F. Baudelet, A. Congeduti, B. Couzinet, and A. Polian, Journal of Physics: Condensed Matter **17**, S883 (2005).

[3] N. Ishimatsu, K. Matsumoto, H. Maruyama, N. Kawamura, M. Mizumaki, H. Sumiya, and T. Irifune, Journal of Synchrotron Radiation **19**, 768 (2012).

[4] Itié, J. P., Polian, A., Martinez, D., Briois, V., Di Cicco, A., Filipponi, A., and San Miguel, A., J. Phys. IV France **7**, C2 (1997).

[5] J.-P. Itie, F. Baudelet, and J.-P. Rueff, X-Ray Absorption and X-Ray Emission Spectroscopy: Theory and Applications **1** (2016).

[6] E. Fonda, A. Rochet, M. Ribbens, L. Barthe, S. Belin, and V. Briois, Journal of Synchrotron Radiation **19**, 417 (2012).

[7] A. San-Miguel, Physica B: Condensed Matter **208**, 177 (1995), proceedings of the 8th International Conference on X-ray Absorption Fine Structure.

[8] A. L. Ankudinov, B. Ravel, J. J. Rehr, and S. D. Conradson, Phys. Rev. B **58**, 7565 (1998).

[9] M. Newville, Journal of Synchrotron Radiation **8**, 322 (2001).

[10] B. Ravel and M. Newville, Journal of Synchrotron Radiation **12**, 537 (2005).
[11] J. J. Rehr, J. J. Kas, F. D. Vila, M. P. Prange, and K. Jorissen, Phys. Chem. Chem. Phys. **12**, 5503 (2010).
[12] P. Giannozzi, S. Baroni, N. Bonini, M. Calandra, R. Car, C. Cavazzoni, D. Ceresoli, G. L. Chiarotti, M. Cococcioni, I. Dabo, *et al.*, J. Phys.: Condens. Matter **21**, 395502 (2009).
[13] J. P. Perdew, K. Burke, and M. Ernzerhof, Phys. Rev. Lett. **77**, 3865 (1996).
[14] J. Klimeš, D. R. Bowler, and A. Michaelides, Phys. Rev. B **83**, 195131 (2011).
[15] J. Klimeš, D. R. Bowler, and A. Michaelides, J. Phys.: Condens. Matter **22**, 022201 (2009).
[16] P. Dalladay-Simpson, J. Binns, M. Peña-Alvarez, M.-E. Donnelly, E. Greenberg, V. Prakapenka, X.-J. Chen, E. Gregoryanz, and R. T. Howie, Nature Communications **10**, 1134 (2019).
[17] A. San Miguel, H. Libotte, J. Gaspard, M. Gauthier, J. Itié, and A. Polian, The European Physical Journal B - Condensed Matter and Complex Systems **17**, 227 (2000).